25th ABCM International Congress of Mechanical Engineering
October 20-25, 2019, Uberlândia, MG, Brazil

COB-2019-1634
RHEOLOGICAL CHARACTERIZATION OF POLYMERIC BLEND FOR ENHANCED OIL RECOVERY (EOR)

Ana Tereza Queiroz de Barros[1]
Rosângela Barros Zanoni Lopes Moreno[2]
School of Mechanical Engineering
University of Campinas– Unicamp
13083-860, Campinas, SP, Brazil

anatrzzz@gmail.com[1], zanoni@fem.unicamp.br[2]

Abstract. *Polymer injection is used by the petroleum industry to improve the oil sweep efficiency in the reservoir, and among the polymer options, partially hydrolyzed polyacrylamide (HPAM) is one of the most commonly used polymers. Recent studies show that the injection of a polymer solution is also capable of mobilizing the residual oil due to the elastic properties of the polymers, turning possible to provide an additional increment of the oil recovery factor. Some authors demonstrated that the molecular weight distribution, often represented by the polydispersity index, directly affects the elastic properties of the polymer. Therefore, the objective of the present work was to optimize the elastic modulus of an HPAM solution through the composition of a polymer blend of the same molecular weight. Rheological tests were performed to determine the apparent viscosity and viscous and elastic modulus of the polymeric solutions prepared with synthetic seawater. The obtained results showed that the polymeric blend presented a higher elastic modulus when compared to the solution with the same average molecular weight made with a single polymer. Also, the polymer blend showed an elastic modulus equivalent to that obtained for the elastic modulus of a single polymer solution of higher molecular weight.*

Keywords: *polymer blends, viscoelasticity, polydispersity index, storage modulus, rheology*

1. INTRODUCTION

About 1.5 trillion barrels of proven crude oil, according to estimates by the Organization of the Petroleum Exporting Countries (OPEC), remains in reservoirs around the world. Enhanced recovery methods not only help in the extraction of residual oil after depletion of conventional methods, but also are responsible for the extraction of residual oil as a source of future economy supply (Al-Hajri et al., 2018). The relevance of polymer injection in oil reservoirs is associated with its ability to improve sweep efficiency through the viscosity increase of the injected fluid and consequent decrease in the water-oil motility ratio.

Recent studies (Xia et al., 2004; Zhang et al., 2010; Wei et al., 2014; Fan et al., 2018) show that in addition to the improvement of the microscopic and volumetric displacement efficiencies, viscoelastic polymer solutions can increase the oil recovery factor due to its elastic properties through the phenomenon called pulling effect. Studies carried out with polymer injections show that when a fluid with elastic properties flows over the microscopic heterogeneities (dead end pores) of a reservoir, normal stresses are generated between the oil and the displacing fluid. That occurs in addition to the shear stresses due to the interfacial interactions between the hydrocarbons present and the injected polymer solution on an atomic scale. Due to the elastic property of the polymer chains, the flow at high velocities through the porous medium generates thickening of the polymer solution. Since the velocity gradient near the surface of the rock is considerably larger for elastic fluids than for Newtonian fluids, a greater force is generated by the injection of viscoelastic polymers. That results in an increase in the oil recovery factor compared to the flooding of non-elastic polymers and purely viscous fluids (Wang et al., 2010, 2011; Fan et al., 2018).

The injection of highly elastic polymer solutions was considered promising as an enhanced recovery method and capable of a significant increase of the oil recovery factor in the Daqing fields. According to Wang et al. (2010; 2011), solutions of very high molecular weight polymers (20-35x106 g/mol) at concentrations of 2000-2500 mg/L showed more satisfactory results than the injection of conventional polymer solutions into those reservoirs: the high viscosity generates a high volumetric sweep efficiency and the high elasticity generates high displacement efficiency, both resulting in an increase in the oil recovery factor. The viscoelasticity and elongation of the partially hydrolyzed polyacrylamide molecules (HPAMs) is assumed to be a property directly proportional to their molecular weight (Wang et al., 2000; Al Hashmi et al., 2013a) and, as the molecular weight increases, higher is its elastic character. However,

several impacts are related to the molecular weight during the injection of polymers into oil reservoirs. For instance, in those cases, mechanical degradation is one of the major factors responsible for the decrease in oil recovery efficiency by polymers (Al Hashmi et al., 2013b).

Many authors have stated that polymer blends with high polydispersity index are an efficient technique to optimize the elastic properties of a polymer solution, without changing the shear viscosity of the solution (Dehghanpour, 2008; Urbissinova, 2010; Urbissinova et al., 2010; Veerabhadrappa et al., 2013). The present work aims to study polymer blends and compare their rheological behavior with a solution prepared with a single polymer and having the same molecular weight or the same elastic properties.

2. EXPERIMENTAL

2.1 Materials

Four anionic HPAMs (AB005-V, 3230-S, 3430-S, and 3630-S) of molecular weights varying from 0.5 x 10^6 g/mol and 20 x 10^6 g/mol and degree of hydrolysis between 25-30% provided by SNF Floerger were selected, as shown in Table 1. Each solution was characterized by different polydispersity indexes. Solutions with a single polymer (pure solution) and made with four polymers in varying concentrations were used as the basis for the analysis of the incremental elastic modulus. The composition of the brine, used to prepare the polymer solutions, was selected based on the literature (Austad et al., 2005; 2008; Lopes, 2017) and aimed at re-creating a synthetic solution of sea water with a concentration of salts of about 33000 mg/L. Table 2 shows the composition of the used synthetic seawater. The pH of the solution (≈ 7,8) was measured with a pH meter (MS Technopon mPA210) at 25.5°C.

Table 1. Description of the polymers used.

Polymer	Molecular Weight (10^6 g/mol)	Anionicity	Degree of Hydrolysis (mol%)
AB005-V	0,5	Very Low	25-30
3230-S	6	Medium to High	
3430-S	12	Medium to High	
3630-S	20	Medium to High	

Table 2. Ionic concentration of the synthetic seawater used in the preparation of the polymer solutions.

Salts	Concentration (g/L)
Na^+	10,345
K^+	0,384
Mg^{2+}	1,194
Ca^{2+}	0,407
Cl^-	18,72
HCO_3^-	0,142
SO_4^{2-}	2,307
Total Dissolved Solids (TDS)	33,50
pH	7,81

2.2 Methodology

2.2.1 Preparation of Solutions

In the present work, solutions with a single polymer (pure solutions) and blends including four polymers in different concentrations were used as the basis for the analysis of the incremental elastic modulus. Solutions with different polymers were prepared in the total polymer concentrations of 2500, 4000 and 5000 mg / L and similar average molecular weight. The 3430-S polymer stock solution (5000 mg / L) (Sample 1) was prepared spreading the polymer pounder in the brine contained in a beaker under stirring on a magnetic stirrer (Fisatom 752A). The vortex was adjusted to approximately 75%. The amount of polymer previously weighed in an analytical scale (OHAUS AV264P) was added to the vortex of the brine and left under low stirring for 24 hours, for complete solubilization. For the stock solution blend (5000 mg / L) (Sample 2), the polymers were uniformly added to the vortex of the brine in decreasing order of molecular weight, i.e. from highest to lowest molecular weight. Then the stirring speed was decreased and the

solution was left under low stirring for 24 hours, until complete solubilization. Dilutions of both solutions, Sample 1 and Sample 2, were performed from the respective stock solutions.

The viscous and elastic moduli are responsible for the behavior of the elongational flow of the polymer molecules through porous media and the molecular weight of the polymer into the solution controls their values. This way, blends can be designed to produce solutions with an average molecular weight distribution equivalent to that for solutions made with a single polymer. The average molecular weight of the mixture was calculated from Equation 1, below:

$$M_{w,B} = \prod_{i=1}^{n} M_{w,i}^{\omega_i} \tag{1}$$

where $M_{w,B}$ is the average molecular weight of the blend, $M_{w,i}$ is the average molecular weight of the i-th polymer and w_i is the mass fraction of the i-th polymer.

The polydispersity index, used as a measure of molecular weight distribution (MWD), was calculated through Equation 2:

$$I = \frac{M_w}{M_n} = \left(\sum_{i=1}^{n} \omega_i M_{w,i}\right)\left(\sum_{i=1}^{n} \frac{\omega_i}{M_{w,i}}\right) \tag{2}$$

where M_w is the average molecular weight and M_n is the number of the average molecular weight. By adjusting the weight fraction of the polymers by the trial and error method, it was possible to arrive at a blend of polymers, Sample 2, of the same average molecular weight as the solution containing a single polymer, Sample 1. Table 3 shows the compositions and indexes of polydispersity for each sample.

Table 3. Composition of polymer solutions.

Solutions	Composition (%)				Average Molecular Weight of the Polymers (10^6 g/mol)	Polidispersity Index
	AB005-V	3230-S	3430-S	3630-S		
Sample 1 (3430-S)	0	0	1	0	12	1,0
Sample 2 (Blend)	0,1	0,1	0,05	0,75	12	4,2

2.2.2 Rheological Analyzes

After mixing and dilute the solutions, rheological analyzes of flow curve, amplitude sweep and frequency sweep were run. The tests were performed at 25.5°C on a rotational rheometer (HAAKE MARS III) using a cone-plate geometry (C35/2° TiL and P35 TiL) with a 0.105 mm gap.

The power-law model, or Ostwald-de Waele equation, describes the viscosity-shear rate relationship and is given by Equation 3 (Sorbie, 1991):

$$\eta = K \cdot \dot{\gamma}^{n-1} \tag{3}$$

where η (Pa.s) is the viscosity, γ (1/s) is the shear rate, K (Pa.s) is the consistency index and n is the fluid behavior index. For n=1, the fluid is Newtonian and the K constant is equivalent to Newtonian viscosity. For 0,4≤n≤1, the fluid is pseudoplastic, i.e., the shear stress is not directly proportional to the rate of shear strain. The determination of the rheological characteristics of a power-law fluid can be performed by the graphical method. In a log-log graph, the values of η and γ fit in a straight line, as shown by Equation 4:

$$ln[\eta] = ln\, K + (n-1) \cdot ln\, \dot{\gamma} \tag{4}$$

The slope of the line gives the value of n and its intersection the value of K.

In dilute polymer solutions, there is a large amount of solute concentrated around the polymer molecule. However, as the polymer concentration increases, the molecules begin to touch each other. At this concentration, called overlap concentration (c*), the solution leaves the diluted regime and enters the semi-diluted regime. The transition between these two regimes is very important from a rheological point of view and is characterized by a change in the shape of the viscosity versus concentration plot. The overlap concentration value is defined by the intersection of the linear slopes in the log-log plot of the viscosity versus concentration of the polymer in solution (Sorbie, 1991; Al-Hashmi, 2013).

Intrinsic viscosity [η] provides information about the viscosity of a given polymer for a certain solvent. Is obtained by plotting the reduced (η_R) and inherent (η_I) viscosities against the polymer concentration and extrapolating the resulting linear curves to the zero polymer concentration. The following equations (5, 6, 7, 8 and 9) are needed for determination of intrinsic viscosity (Sorbie, 1991):

$$[\eta] = \lim_{c \to 0} \eta_R \tag{5}$$

or

$$[\eta] = \lim_{c \to 0} \eta_I \tag{6}$$

where:

$$\eta_R = \frac{\eta - \eta_S}{c \cdot \eta_S} \tag{7}$$

$$\eta_I = \frac{ln\, \eta_r}{c} \tag{8}$$

$$\eta_r = \frac{\eta}{\eta_S} \tag{9}$$

where η (mPa.s) is the polymer solution viscosity, η_R is the reduced viscosity, η_S (mPa.s) is the solvent viscosity, η_I is the inherent viscosity, ηr is the relative viscosity, and c (mg/L) is the polymer concentration.

The Mark-Houwink equation, Equation 10, correlates the intrinsic viscosity with molecular weight. Both the constants *K'* and *a* vary with polymers, solvents and temperature.

$$[\eta] = K' \cdot M^a \tag{10}$$

[η] is the intrinsic viscosity (cm^3/g), M (g/mol) is the molecular weight of the polymer and K' (cm^3/g), and *a* are the constants for a given solute-solvent system. The graphic representation of Equation 11 gives the calculation of Mark-Howink parameters:

$$ln[\eta] = ln[K^{'}] + a \cdot ln[M] \tag{11}$$

Using values obtained from [η] in the same solvent and at the same temperature for several HPAM samples with known molecular weights, it is possible to obtain the values of parameters *a* and K'. A graph of ln [η] versus ln [M] usually provides a straight line. The slope of this line represents the value of *a* and its interception, the value of ln [K']. Masuelli (2014) describes that a long-chain polymer molecule in solution assumes a kinked or coiled shape and a rigid linear configuration. The author defines that the value of Mark-Houwink "*a*" constant in the range between 0,8 – 2,0 represents a rigid configuration of the polymer chain, such as a rod (stiff chain).

Newton's Law (Equation 12) is responsible for the definition of a purely viscous fluid. An analogous to Newton's Law for purely elastic fluids is Hooke's Law (Equation 13).

$$\tau = \eta \cdot \dot{\gamma} \tag{12}$$

$$\tau = G \cdot \gamma \tag{13}$$

where τ is the stress, γ is the strain and G is the modulus of rigidity.

Oscillatory tests, which involve the application of small oscillatory deformations, are used to measure the viscoelastic properties of a given material. A stress is applied to the material and the observed strain will present some temporal discrepancy with respect to the stress. Figure 1 shows the sinusoidal variation of strain and stress as a function of time. Sinusoidally oscillating shear strain produces a sinusoidal stress phase shifted by a phase angle, δ.

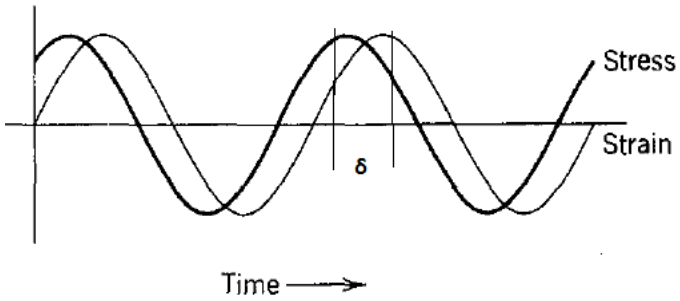

Figure 1: Sinusoidal variation of strain and stress as a function of time
(Adapted from Ferry, 1980)

The stress is related to the strain through the complex modulus, G*, which measures the resistance of the material to a given applied strain. The part of the strain that is in phase with stress, and which elastically follows the application of stress, is represented by a storage modulus, or elastic modulus, G '. The other part, which is out of phase, is represented by a loss modulus, or viscous modulus, G ". Equations 14, 15 and 16 present the relationships between these parameters (Ferry, 1980; Macosko, 1994).

$$G^* = G' + iG'' \tag{14}$$

$$G' = G^* \cdot \cos\delta \tag{15}$$

$$G'' = G^* \cdot \sin\delta \tag{16}$$

G' describes the elastic storage of energy of the sample, while G'' describes the viscous dissipation due to permanent deformation under flow. Amplitude sweep and frequency sweep are oscillation tests that measure viscoelastic properties of materials. Amplitude sweep tests show the dependence of modules G' and G'' when subjected to progressive shear stress, providing a response from the internal structure of the sample. This test defines the region of linear viscoelastic response (LVR) of the sample and a stress value inside the LVR is selected and used in frequency sweep test. The frequency sweep test measures viscoelastic properties of the sample as a function of frequency.

2.3 Results and Discussions

Under low shear rates, the HPAM molecules are in solution as spherical coils and there are no forces to stretch the polymer coil, so that, the solution exhibits a Newtonian behavior and the apparent viscosity is equal to the shear viscosity. However, when the rate increases, loss of shear viscosity occurs, resulting in the appearance of pseudoplastic rheology (Zhang et al., 2010). The flow curves obtained for the solutions showed that both blends and the solution with a single polymer at the same concentrations presented the same viscous characteristics and pseudoplastic rheology. Figure 2 shows the apparent viscosity versus shear rate, and Tab. 4 summarizes the power-law parameters. The viscosities obtained for the shear rate of 7.8 s^{-1} at the concentrations of 2500, 4000 and 5000 were approximately 30, 90 and 130 mPa.s, respectively.

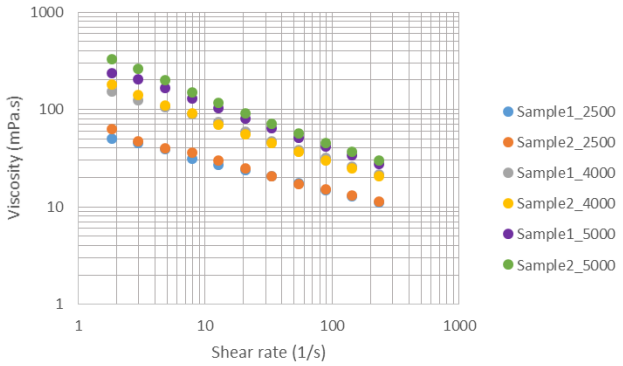

Figure 2. Flow curves obtained for 3430-S solutions (Sample 1) and Blend (Sample 2)

Table 4. Power-law parameters obtained for solutions at 25,5°C

Concentrations	Sample 1			Sample 2		
	n	K	R^2	n	K	R^2
2500	0.685	61.68	0.998	0.653	71.64	0995
4000	0.592	199.7	0.999	0.549	227.6	0.998
5000	0.542	327.59	0.998	0.501	429.12	0.998

Comparing the overlap concentrations for solutions with the same average molecular weight (Figures 3 and 4), one can observe that the solution with the highest polydispersity index, Sample 2, reaches a critical concentration in a lower value than the solution containing a single polymer and with a lower polydispersity index, Sample 1.

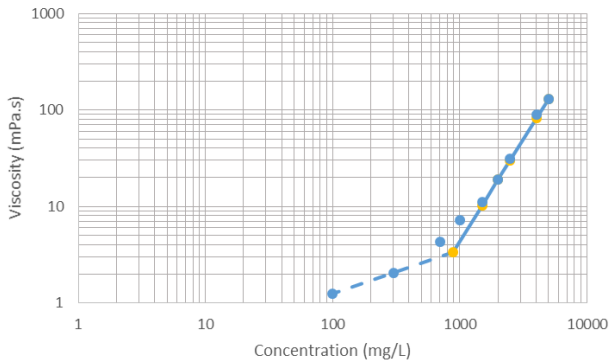

Figure 3. Overlap Concentration of Sample 1

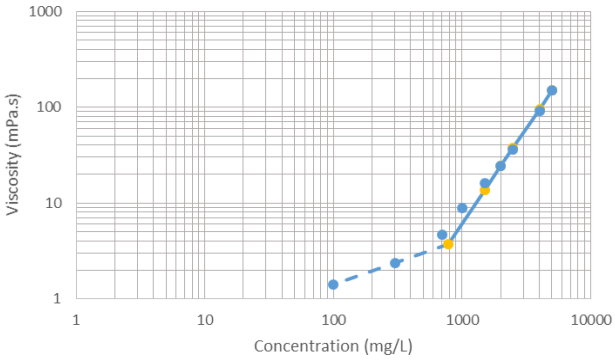

Figure 4. Overlap Concentration of Sample 2

The values obtained for Sample 1 and Sample 2 were approximately 885 mg/L and 780 mg/L, respectively. The difference between the overlap concentration values for the solutions of the same average molecular weight can be explained by the greater entanglement caused by the mixture of polymer molecules of different sizes and molecular weights present in Sample 2. That increases the intermolecular interactions in the solution.

The curves obtained for the reduced and inherent viscosities of Sample 1 and Sample 2 (7.8 s -1) as a function of the concentration of polymers in the diluted region are presented in Figures 5 and 6. In those figures, the intrinsic viscosities [η] for both solutions were obtained by extrapolating the linear curves to a zero concentration of polymers and their values were found approximately 2600 cm^3/g and 3400 cm^3/g for Sample 1 and Sample 2 at 25.5°C, respectively.

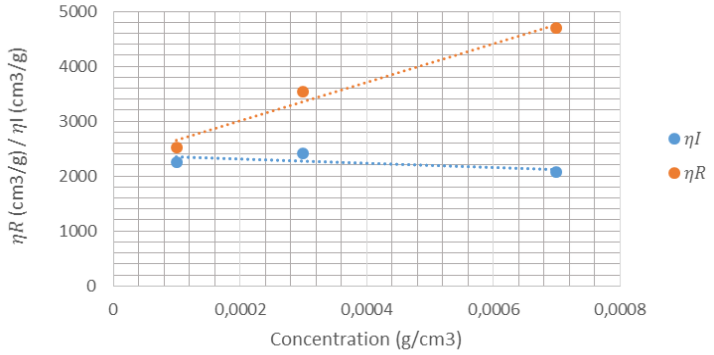

Figure 5. Determination of intrinsic viscosity for Sample 1 at 25.5 ° C

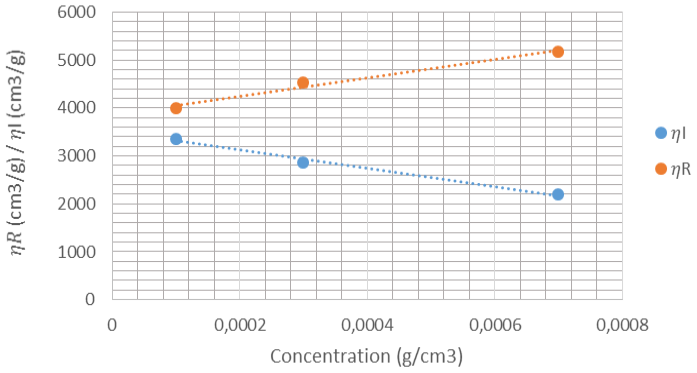

Figure 6. Determination of intrinsic viscosity for Sample 2 at 25.5 ° C

From the [η] value calculated for sample 1 (single polymer solution, 3430-S) and previous values of [η] obtained for solutions of polymers 3230-S and 3630-S under the same salinity and temperature conditions, it was possible to set values for the K' and *a* Mark-Houwink parameters. Figure 7 represents the graph of ln [η] versus ln [M] and the straight line obtained.

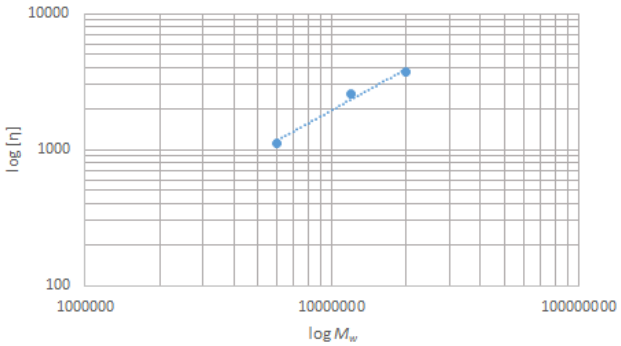

Figure 7: Graph of ln [η] versus ln [M] for determining Mark-Houwink parameters

For HPAM polymer solutions using synthetic seawater (33500 mg/L) as a solvent at a temperature of 25,5°C, the parameters *a* and K' found were 1,0 and $0{,}2x10^{-3}$ cm^3/g, respectively.

For the analysis of the behavior of the elastic modulus (G ') of the solutions with the increase of the shear stress, amplitude sweep tests were carried out at the frequency of 1 Hz and a tension range delimited between 0.013 and 2.06 Pa. Based on the analysis of the data obtained for the amplitude sweep tests, a tension of 0.1 Pa was established for the frequency sweep tests. For all concentrations and solutions analyzed, this tension was within the region of linear viscoelasticity and corresponded to the maximum tension value for the linear viscoelastic response of polymer solutions (Dehghanpour, 2008). Figure 8.(a) shows the results obtained in amplitude sweep tests for the elastic moduli of both solutions. Figure 8.(b) shows the results obtained for the elastic modulus during the frequency sweep tests of both samples.

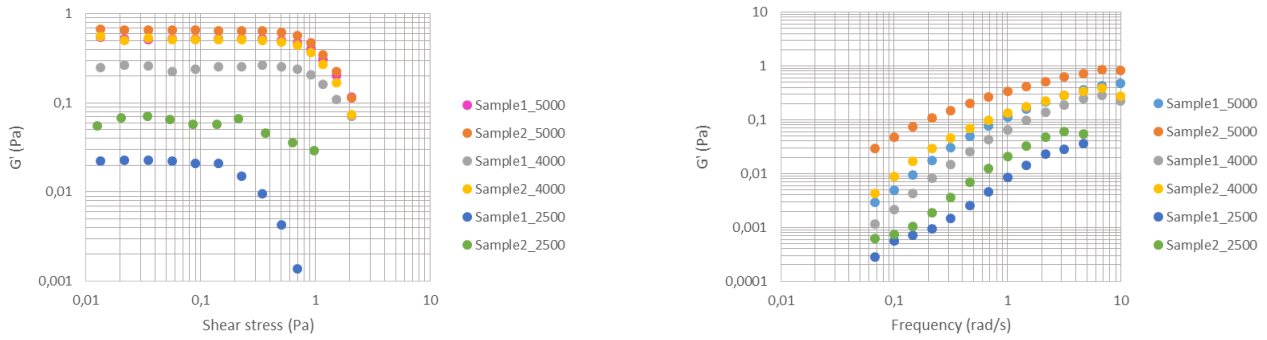

Figure 8. a) G' modulus obtained in amplitude sweep tests and b) G' modulus obtained in frequency sweep tests.

In Figure 8 (a), at the highest concentration (5000 mg/L of HPAM), the samples presented elastic modulus slightly higher than that presented by the solution of a single polymer. However, as the concentration of solutions decreased, this difference became more pronounced. The region of linear viscoelasticity could be observed between 10^{-2} to 10^{-1} Pa. In that region, the elastic modulus G' does not depend on the applied deformation and the internal structure of the system is preserved. The found interval, of amplitude is generally used in linear oscillatory shear tests for polymer solutions. The data determined in this work for the G' modulus agreed with those obtained by Urbissinova (2010) and Urbissinova et al. (2010). They carried out amplitude sweep tests to analyze the influence of the polydispersity index using polymer blends of the same average molecular weight in deionized water. The authors associated the difference in the elastic modulus of each solution with the polydispersity indexes: the higher the polydispersity index of the solution, higher is its elastic structure and, consequently, its elastic modulus.

In Figure 8 (b) is observed that for the concentrations of 2500 and 4000 mg/L of both samples, the elastic modulus obtained in each concentration were almost the same for the samples 1 and 2. At the concentration of 5000 mg/L, it was observed that the G' of both samples become closer at higher frequencies. Veerabhadrappa et al. (2013) also found similar behavior during the evaluation of G' in frequency sweep tests. For the HPAM blends analyzed by the authors, elastic modulus tended to be closer to each other the higher the frequency.

Finally, flow curve, amplitude sweep and frequency sweep tests were performed for a very high molecular weight HPAM solution ($20x10^6$ g/mol) at a concentration of 2500 mg/L and under the same conditions. The results obtained were compared with the results of samples 1 and 2 at the same concentrations. Figure 9 (a) shows the apparent viscosity versus shear rate for the polymer 3630-S, Sample 1 and Sample2; and Figure 9 (b) shows the results obtained in amplitude sweep tests (1 Hz of frequency and tension range delimited between 0,013 and 2,06 Pa) for the elastic modulus of the three solutions.

Figure 9. a) Flow curve results and b) G' modulus obtained in amplitude sweep tests.

In Figure 9 (a) it is observed that at shear rates close to 10 mPa.s, the viscosity of the 3630-S polymer solution comes close to the viscosity of Samples 1 and 2. The Figure 9 (b) shows that the G' value for the 3630-S polymer solution and Sample 2 are very close, while Sample 1 has a G' value far below the values of the other two solutions.

Figure 10 shows the results of frequency sweep tests for (a) the viscous modulus and (b) the elastic modulus of the three solutions analyzed (with a tension of 0.1 Pa established).

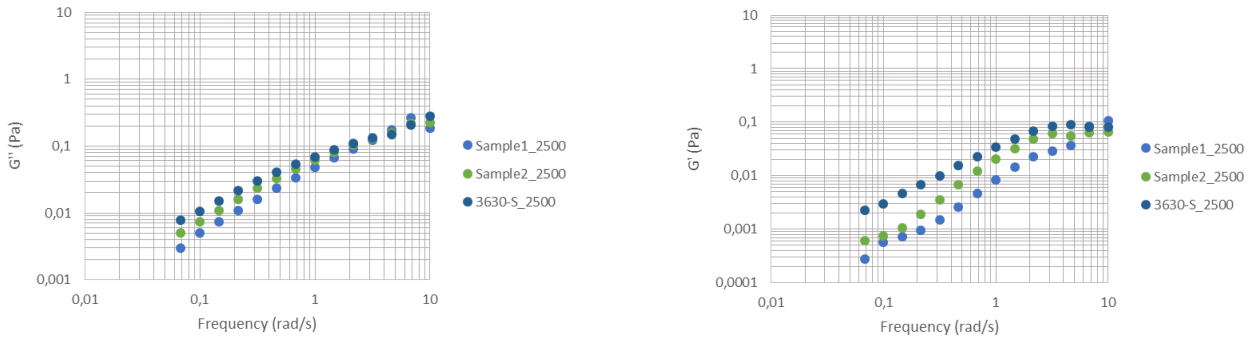

Figure 10. a) G'' modulus obtained in frequency sweep tests and b) G' modulus obtained in frequency sweep tests.

The solution with the highest polydispersity index, Sample 2, and the polymer 3630-S solution showed almost identical viscous modules, as shown in Figure 10.(a). At frequencies above 0.9 rad/s, Figure 10.(b), Sample 2 and 3630-S polymer solution showed almost similar elastic modulus, even with the large molecular weight difference between the respective polymeric solutions. This similarity in the G' value was not observed between the solutions of Sample 1 and 3630-S.

2.4 Conclusions

The results showed that polymer blends diluted in synthetic sea water and with a high polydispersity index could optimize the elastic modulus to such an extent that it is equivalent to the module of solutions with a polymer of very high molecular weight. The difference in the capacity of displacement of the oil by polymers of different molecular weights is related to the viscoelastic properties, especially the elastic ones. Thus, by obtaining the same elastic character for a lower molecular weight molecule, an increase in residual oil recovery can be achieved by reducing the impacts caused by the mechanical degradation during the flow in porous media of high molecular weight polymers.

3. ACKNOWLEDGEMENTS

The authors would like to acknowledge the Graduate Program in Petroleum Sciences and Engineering (CEP-FEM-Unicamp), Laboratory of Oil Reservoirs (Labore-Unicamp) and SNF-Floerger for provided polymer samples. We also wish to recognize the financial support provided by the Coordination of Improvement of Higher Education Personnel (CAPES).

4. REFERENCES

Al Hashmi. A.R., Al Maamari, R.S., Al Shabibi, I.S., Mansoor, A.M., Zaitoun, A., Al Sharji, H.H. 2013. Rheology and mechanical degradation of high-molecular-weight partially hydrolyzed polyacrylamide during flow through capillaries. *Journal of Petroleum Science and Engineering*. Vol.105. pp.100-106.

Al-Hajri, S., Mahmood, S.M., Abdulelah, H., Akbari, S. 2018. An overview on polymer retention in porous media. *Energies*. Vol. 11, No. 2751. doi:10.3390/en11102751

Austad, T., Strand, S., Hogneses, E.J., Zhang, P. 2005. Seawater as IOR fluid in fractured chalk. In: SPE International Simposium on Oilfield Chemistry, 2-4 February, Woodland, Texas, USA.

Austad, T., Strand, S., Madland, M.V., Puntervold, T., Korsnes, R.I. 2008. Seawater in Chalk: An EOR and compaction fluid. *SPE Reservoir Evaluation & Engineering*, Vol.11, No. 4, pp. 648-654.

Dehghanpour, H.A. 2008. Investigation of viscoelastic properties of polymer based fluids as a possible mechanism of internal filter cake formation. MS. thesis, University of Alberta, Edmonton, Alberta, Canada.

Fan, J.C., Wang, F.C., Chen, J., Zhu, Y.B., Lu, D.T., Liu, H., Wu, H.A. 2018. Molecular mechanism of viscoelastic polymer enhanced oil recovery in nanopores. *Royal Society Open Science*. 5:180076. DOI: http://dx.doi.org/10.1098/rsos.180076.

Ferry, J.D. 1980. *Viscoelastic Properties of Polymers*. John Wiley & Sons, Inc. Canada.

Lopes, L.F. 2017. Recuperação de petróleo por injeção de solução polimérica em rochas carbonáticas com monitoramento da frente de saturação. Ph.D.thesis, Unicamp, Campinas, São Paulo, Brasil.

Macosko, C.W. 1994. *Rheology: Principles, Measurements and Applications.* Wiley-VCH, Inc., Canada.

Masuelli, M.A. 2014. Mark-Houwink parameters for aqueous-soluble polymers and biopolymersnat various temperatures. *Journal of Polymer and Biopolymer Physics Chemistry*. Vol.2, No.2, pp. 37-43.

Sorbie, K.S. 1991. *Polymer-Improved Oil Recovery*. Blackie, CRC Press, Florida, 1st edition.

Urbissinova, T.S. 2010. Experimental investigation of the effect of elasticity on the sweep efficiency in viscoelastic polymer flooding operations. MS. thesis, University of Alberta, Edmonton, Alberta, Canada.

Urbissinova, T.S., Trivedi, J.J., Kuru, E. 2010. Effect of elasticity during viscoelastic polymer flooding: a possible mechanism of increasing the sweep efficiency. *Journal of Canadian Petroleum Technology*. Vol.49, No. 12, pp. 49-56.

Veerabhadrappa, S.K., Trivedi, J.J., Kuru, E. 2013. Visual confirmation of the elasticity dependece of unstable secondary polymer floods. *Industrial and Engineering Chemical Research*. Vol. 12, No. 18, pp. 6234-6241.

Wang, D., Cheng, J., Yang, Q., Gong, W., Li, Q., Chen, F. 2000. Viscous-elastic polymer can increase microscale displacement efficiency in cores. In: SPE Annual Technical Conference and Exhibition, 1-4 October, Dallas, Texas.

Wang, D., Xia, H., Yang, S., Wang, G. 2010. The influence of visco-elasticity on micro forces and displacement efficiency in pores, cores and in the field. In: SPE EOR Conference at Oil&Gas West Asia, 11-13 April, Muscat, Oman.

Wang, D., Wang, G., Xia, H. 2011. Large scale high viscous-elastic fluid flooding in the field achieves high recoveries. In: SPE Enhanced Oil Recovery Conference, 19-21 July, Lumpur, Malaysia.

Wei, B., Romero-Zéron, L., Rodrigue, D. 2013. Oil displacement mechanisms of viscoelastic polymers in enhanced oil recovery (EOR): a review. *Journal of Petroleum Exploration and Production Technology*. Vol.4, No.2, pp. 113-121.

Xia, H., Wang, D., Wu, J., Kong, F. 2004. Elasticity of HPAM solutions increases displacement efficiency under mixed wettability conditions. In: SPE Asia Pacific Oil and Gas Conference and Exhibition, 18-20 October, Perth, Australia.

Zhang, Z., Li, J., Zhou, J. 2010. Microscopic roles of viscoelasticity in HPAM polymer flooding for EOR. *Transport in Porous Media*. Vol.86, No.1, pp. 199-214.

5. RESPONSIBILITY NOTICE

The authors are the only responsible for the printed material included in this paper.